International Journal of Mathematical Archive-10(6), 2019, 19-31
Available online through www.ijma.info ISSN 2229 – 5046

HALL EFFECT ON MHD HEAT AND MASS TRANSFER OF A NANOFLUID OVER A STRETCHING SHEET WITH PARTIAL SLIP

ANJNA SINGH*
Professor, Department of Mathematics,
Government Girls P.G. College, Rewa-486001, Madhya Pradesh, India.

(Received On: 10-05-19; Revised & Accepted On: 15-06-19)

ABSTRACT

T*he present investigation deals with the boundary layer flow, heat and mass transfer of nanofluid over a stretching sheet under the influence of an Hall current. Similarity transformations are used to convert the governing partial differential equations into a system of non-linear ordinary differential equations and are solved numerically by using shooting method. The effects of magnetic field, Hall parameter, Brownian motion parameter, thermophoresis parameter, Prandtl number on the velocity, temperature and concentration fields are discussed numerically through graphs and tables.*

Keywords: *Hall effect, MHD, Heat and Mass transfer, Stretching Sheet, Nano fluid.*

1. INTRODUCTION

Study of convective heat transfer in nanofluids has become a topic of contemporaneous interest due to its applications in several industries such as power plant operations, manufacturing and transportation, electronics cooling, heat exchangers. The word "nanofluid" coined by Choi (1995) refers to a liquid suspension containing ultra - fine particles (diameter less than 50 nm). The traditional fluids used for heat transfer applications such as water, mineral oils, ethylene glycol, engine oil have limited heat transfer capabilities. The nanofluids which are the engineered colloidal suspension of nano meter sized particle of metals and metallic oxides such as aluminum, copper, gold, iron and titanium or their oxides in base fluids. The base fluids are usually water, oil, ethylene glycol, bio fluids and toluene. Experimental investigations revealed that base fluids with suspension of the nanoparticles have substantially higher thermal conductivities than those of the base fluids. Eastman *et al.* (2001) and Minsta (2009) showed that even with small volumetric fraction of nanoparticles (less than 5%), the thermal conductivity of the base liquid can be enhanced by 10 - 50%. It was reported that a small amount (less than 1% volume fraction) of copper nanoparticles or carbon nanotubes dispersed in ethylene glycol or oil can increase their inherently poor thermal conductivity by 40% and 50%, respectively (Eastman *et al.*, 2001; Choi *et al.*, 2001). The unique properties of these nanofluids made them potential to use in many applications in heat transfer. A recent application of the nanofluid as suggested by Kleinstreuer *et al.*, (2008) is in delivery of nano-drug. Eastman *et al.*, (1997) attributed the enhancement of thermal conductivity to the increase in surface area due to the suspension of nanoparticles. Keblinski *et al.*, (2002) discussed on the possible mechanisms for the improved thermal conductivity. According to them the contribution of Brownian motion is much less than other factors such as size effect, clustering of nanoparticles and surface adsorption. Boungiorno (2006) evaluated the different theories explaining the enhanced heat transfer characteristics of nanofluids. He developed an analytical model for convective transport in nanofluids which takes into account the Brownian diffusion and thermophoresis. Using this model, Kuznetsov and Nield (2010) investigated the natural convective flow of a nanofluid over a vertical plate. Bachok *et al.* (2010) numerically studied steady boundary layer flow of a nanofluid over a moving semi-infinite plate in a uniform free stream. Effect of magnetic fuel on free convection flow of a nanofluid past a vertical semi-infinite flat plate has been discussed by Hamad *et al.* (2011). Gorla and Chamkha (2011) investigated natural convection flow past a horizontal plate in a porous medium filled with a nanofluid. The fluid flow due to a stretching surface has important applications such as production of glass and paper sheets, metal spinning, hot rolling, drawing of plastic films, and extrusion of metals and polymers. Khan and Pop (2010) studied the boundary layer flow of a nanofluid past a stretching sheet. Vajravelu *et al.* (2011) analyzed the convective heat transfer of Ag-water and Cu-water nanofluids over a stretching surface. The heat and mass transfer analysis for boundary layer stagnation – point flow over a stretching sheet in a porous medium saturated by a nanofluid with internal heat generation/absorption and

Corresponding Author: Anjna Singh*
Professor, Department of Mathematics,
Government Girls P.G. College, Rewa-486001, Madhya Pradesh, India.

suction/blowing is investigated by Hamad and Ferdows (2011). Nadeem and Lee (2012) made an analytical investigation of the problem of steady boundary layer flow of a nanofluid over an exponential stretching surface including the effects of Brownian motion and thermophoresis. Makinde and Aziz (2011) studied the boundary layer flow of a nanofluid past a stretching sheet with a convective boundary condition. Rana and Bhargava (2011) analyzed numerically the flow and heat transfer of a nanofluid over a nonlinearly stretching sheet.

The study of magnetohydrodynamics has significant applications in engineering. MHD generators, devices in petroleum industry, material processing, nuclear reactors etc are some applications. The use of magnetic fields plays an important role in the process of purification of molten metals from non metallic inclusions. When a strong magnetic field is applied to an ionized gas with low density, the conductivity normal to the magnetic field is reduced owing to the free spiraling of electrons and ions around the magnetic lines of force and the current is induced in the normal direction to the electric and magnetic fields. This effect is known as the Hall Effect. The study of MHD heat transfer with Hall currents has several engineering applications for example power generators, transmission lines, refrigeration coils, MHD accelerators, electric transformers etc. Several researchers studied the effect of Hall currents on MHD boundary layer flow. Abo-Eldahab and Elbarbary (2001) analyzed the effect of Hall current on magnetohydrodynamic free convection flow past a semi-infinite vertical plate with mass transfer. Abo-Eldahab and Abd El-Aziz (2000) investigated the effect of Hall and ion-slip currents with temperature-dependent internal heat generation or absorption on MHD free convection flow past a semi-infinite vertical flat plate. Hall effect on MHD mixed convection boundary layer flow over a stretched vertical flat plate was studied by Ali *et al.* (2011). Abo-Eldahab and Salem (2004) considered the Hall Effect on MHD free convection flow of a non-Newtonian power-law fluid over a stretching surface. Abd El-Aziz (2010) has reported that the effects of Hall currents on the flow and heat transfer of an electrically conducting fluid over an unsteady stretching surface in the presence of strong magnetic field. Magnetic nanofluid has both the liquid and magnetic properties. These fluids have been used in magneto-optical wavelength filters, optical gratings, optical switches etc. The study of Hall effects on nanofluid has applications in MHD energy generators. Study on the problem of Hall currents in nanofluids over a stretching sheet are very limited. Xiaohonh Su and Liancun Zheng (2013) studied the Hall effect on MHD flow and heat transfer of nanofluids over a stretching wedge in the presence of velocity slip and Joule heating. Four different types of water-based nanofluids containing copper (Cu), silver (Ag), alumina (Al2O3), and titania (TiO2) nanoparticles are investigated. Mohamed Abd El-Aziz (2013) analyzed the effects of Hall current on the steady boundary layer MHD slip flow over a stretching sheet in a water-based nanofluid containing different types of nanoparticles: Cu, Al2O3 and Ag. In this paper we analyzed the Hall effect on the MHD boundary layer flow and heat transfer of nanofluids over a stretching sheet. Using the model developed by Boungiorno the effect of buoyancy ratio number, Hall current parameter, magnetic field, Brownian motion parameter, thermophoresis parameter, Prandtl number and Lewis number on the velocity, temperature and volume fraction of nanopaticles is discussed.

2. MATHEMATICAL FORMULATION

Consider the steady flow of an electrically conducting incompressible nanofluid past a stretching flat surface located at y = 0 (Fig. 1) with a velocity proportional to the distance from the fixed origin O of a stationary frame of reference (x, y, z). We choose the frame of reference (x, y, z) such that positive x coordinate is measured along the stretching sheet in the direction of motion of the stretching surface, the y coordinate is measured in the direction normal to this surface and z – axis is transverse to the xy – plane.

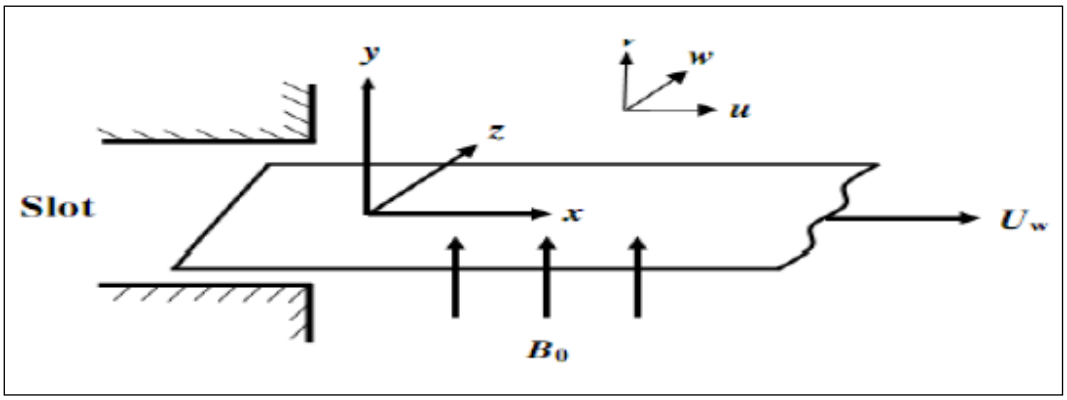

Fig.-1: Physical model and coordinate system

We consider that an external constant magnetic field B0 is applied in the positive y – direction. The temperature and the nanoparticle fraction are maintained at prescribed constant values Tw and Cw on the sheet while the ambient fluid has a uniform temperature T∞ and concentration C∞. Taking Hall effects into account and assuming that the electronic pressure is neglected and no electric field is imposed on the flow field, the generalized Ohm's law that includes Hall current Sutton and Sherman (1965) can be written as

$$\bar{J} = \sigma\left(\bar{E} + \bar{V}x\bar{B} - \frac{1}{en_e}\right)x\bar{B} + \frac{1}{en_e}\nabla p_e \tag{1}$$

Where $\bar{J} = (J_x J_y, J_z)$ is the current density vector,E is the intensity vector of the electric field,V is the velocity vector, $\bar{B} = (0, B_0, 0)$ the magnetic induction vector, $\sigma(= e^2 n_e t_e / m_e)$ is the electrical conductivity,τe is the electron collision time,e is th rcharge of elec tron,ne is the number of density of electrons,me is mass of the electrons and Pe the electron pressure .The equation of conservation of electron charge $\nabla.\bar{J} = 0$ resuults $j_y = cons\tan t$,this indicates that $j_y = 0$ everywhere in the flow .

Hence equation (1) reduces to

$$j_x = \frac{\sigma B_0}{1+m^2}(mu - w) \tag{2}$$

$$j_z = \frac{\sigma B_0}{1+m^2}(u + mw) \tag{3}$$

Here u, v and w are the components of the velocity vector V, m=(=$\omega_e\tau_e$) is the Hall parameter,ω e is the electron frequency.

We assume that the nanofluid is isotropic and homogeneous and has the constant viscosity and electric conductivity. Under these assumptions and the equations (2) and (3) the boundary layer equations governng this MHD flow, heat and mass transfer of nanofluids with Hall effect using Boussinesq approximation are

$$\frac{\partial u}{\partial x} + \frac{\partial v}{\partial y} = 0 \tag{4}$$

$$u\frac{\partial u}{\partial x} + v\frac{\partial u}{\partial y} = \frac{\partial^2 u}{\partial y^2} + \frac{1}{\rho_e}[(1-C_\infty)\rho_{f_\infty}\beta g(T-T_\infty)] - \frac{(\rho_p - \rho_{f_\infty})g(C-C_\infty)}{\rho_f} - \frac{\sigma B_o^2}{\rho_f(1+m^2)}(u+mw) \tag{5}$$

$$u\frac{\partial w}{\partial x} + v\frac{\partial w}{\partial y} = \frac{\partial^2 w}{\partial y^2} + \frac{\sigma B_o^2}{\rho_f(1+m^2)}(mu - w) \tag{6}$$

$$u\frac{\partial T}{\partial x} + v\frac{\partial T}{\partial y} = \frac{k_f}{\rho_f C_p}\frac{\partial^2 T}{\partial y^2} + \tau\left[D_B\frac{\partial T}{\partial y}\frac{\partial C}{\partial y} + \frac{D_T}{T_\infty}\left(\frac{\partial T}{\partial y}\right)^2\right] + Q_1^1(C-C_\infty) - \frac{\partial(q_R)}{\partial y} - Q_H(T-T_\infty) \tag{7}$$

$$u\frac{\partial C}{\partial x} + v\frac{\partial C}{\partial y} = D_B\frac{\partial^2 C}{\partial y^2} + \frac{D_T}{T_\infty}\left(\frac{\partial^2 T}{\partial y^2}\right) - K_C(C-C_\infty) \tag{8}$$

where $\nu, \rho_f, \rho_p, g, \beta, B_o, T, C, k_f C_p, \tau = (\rho C_p)_p/(\rho C_p)_f, D_B, D_T$, Q_1^1 ,Q_H and q_R are the kinematic viscosity, density of the base fluid,nanoparticle density, gravitational force due to acceleration, coefficient of thermal expansion,magnetic field of constant strength,temperature,concentration of the nanofluid,coefficient of thermal diffusivity,ratio of nanoparticle heat capacity and base fluid heat capacity, Brownian diffusion coefficient, thermophoretic diffusion coefficient, Strength of the Heat source, Radiative heat flux.

The boundary conditions for the velocity, temperature and concentration fields for the problem are

$$u = U_w = bx, v = w = 0, T = T_w, C = C_w \quad \text{at y=0} \tag{9}$$

$$u = w = 0, T = T_\infty C = C_\infty \text{ as } \quad y \to\infty \tag{10}$$

Where Uw=bx, b>0. The boundary conditions on the velocity are no-slip conditions at the surface y=0, while the boundary conditions on the velocity as y→∞ follows from the fact that there is no flow far away from the stretching sheet.The temperature and nanoparticle

Concentration are maintained at a prescribed constant values Tw and Cw at the sheet and are assumed to vanish far away from the sheet.

Invoking Rosseland approximation, the radiative flux q_r is $q_r = \frac{-4\sigma_s}{3K_e}\frac{\partial T^{1^4}}{\partial y}$, and lineralized by expanding T^{1^4} into

Taylor series about $T_\infty^{\ 1}$ which after neglecting higher order terms and takes the form $T^{1^4} \cong 4T_\infty^{\ 1^3}T^1 - 3T_\infty^{\ 1^4}$.

With this the energy equation reduces to

$$\rho C_p\left(u\frac{\partial T}{\partial x}+v\frac{\partial T}{\partial y}\right)=k_f\frac{\partial^2 T}{\partial y^2}+\tau\left[D_B\frac{\partial T}{\partial y}\frac{\partial C}{\partial y}+\frac{D_T}{T_\infty}\left(\frac{\partial T}{\partial y}\right)^2\right]+Q_1^1(C-C_\infty)+\frac{16\sigma^* T_\infty^3}{3\beta_R}\frac{\partial^2 T}{\partial y^2}-Q_H(T-T_\infty) \quad (11)$$

Introducing the following similarity transformations

$$u=bxf'(\eta),v=-\sqrt{b\nu}\,f(\eta),w=bxg(\eta),$$
$$\eta=\sqrt{\frac{b}{\nu}}y,\theta(\eta)=\frac{T-T_\infty}{T_w-T_\infty},\phi-\frac{C-C_\infty}{C_w-C_\infty} \quad (12)$$

On introducing equations (12) into equations (5)-(8) & (11), we get the following ordinary differential equations

$$f'''+ff''-(f')^2+G(\theta-Nr\phi)-\frac{M}{1+m^2}(f'+mg)=0 \quad (13)$$

$$g''+fg'-f'g+\frac{M}{1+m^2}(mf'-g)=0 \quad (14)$$

$$\left(1+\frac{4Rd}{3}\right)\theta''+\Pr\, f\theta'+\Pr\, Nb\varphi'\theta'+\Pr\, Nt(\theta')^2-Q\theta+Q_1\varphi=0 \quad (15)$$

$$\varphi''+\left(\frac{Nt}{Nb}\right)\theta''+Le(f\varphi')-Le\,\gamma\,\varphi=0 \quad (16)$$

Subject to the boundary conditions

$$f'(0)=1,f(0)=0,g(0)=0,\theta(0)=1,\phi(0)=1 \qquad at\ \ \eta=0 \quad (17)$$

$$f'(\infty)=g(\infty)=\theta(\infty)=\phi(\infty)=0 \quad as \quad \eta\to\infty \quad (18)$$

where the prime denote differentiation with respect to η.The non-dimensional parameters

$G=\frac{Gr_x}{\mathrm{Re}_x^{\,2}}$ (Mixed convection parameter), $Gr_x=\frac{\beta g(T_w-T_\infty)x^3}{\nu^2}$ (local Grashof number)

$\mathrm{Re}_x=\frac{xU_w(x)}{\nu}$ (local Reynolds number), $Nr=\frac{(\rho_p-\rho_{f_\infty})(C_w-C_\infty)}{(1-C_\infty)\rho_{f\infty}\beta(T_w-T_\infty)}$ (buoyancy ratio number),

$Nb=\frac{(\rho C)_p D_B(C_w-C_\infty)}{\nu(\rho C)_f}$, (Brownian motion parameter), $M=\frac{\sigma B_0^2}{\rho b}$, (Magnetic parameter), $Q=\frac{\mu Q_H}{bC_p}$

(Heat source parameter), $Rd=\frac{4\sigma^* T_\infty^3}{k_f\beta_R}$ (Thermal radiation parameter), $Q_1=\frac{Q_1^1(Cw-C_\infty)}{\rho C_p b(Tw-T_\infty)}$ (Radiation absorpton parameter), $Nt=\frac{(\rho C)_p D_T(T_w-T_\infty)}{\nu(\rho C)_f T_\infty}$, (Thermophoresis motion parameter), $Le=\frac{\nu}{D_B}$, (Lewis number),

$\gamma=\frac{K_C}{b}$ (Chemical reaction parameter), $\Pr=\frac{\mu C_p}{k_f}$ (Prandtl number)

3. RESULTS AND DISCUSSION

The non-linear ordinary differential equations (12) – (15) subject to the boundary conditions (16) & (17) are solved numerically using the shooting technique. In order to verify the validity and accuracy of the numerical scheme applied in the present analysis, results for the heat transfer rate $\theta'0$ for different values of Prandtl number have been compared with the published results of *Grubka* & *Bobba* [16] and *Ali* [6] for regular viscous fluid over a linearly stretching sheet in the absence of magnetic field (M=0), Hall current (m=0). The results are found to be in good agreement as presented in Table (1).

Table-1: Comparison of the values of wall temperature gradient -θ' (0) with those of Grubka and Bobba (16), Ali (6), M. Abd El-Aziz (2) when λ= Nr = M = m = Nb = Nt = Le = 0

Pr	Grubka and Bobba [16]	Ali [6]	M. Abd El-Aziz [2[	**Present results -θ' (0)**
0.01	0.0197	-	0.01973	**0.01969**
0.72	0.8086	0.8058 0.9961	0.80868	**0.80761**
1.0	1.0000	1.9144 3.7006	1.00001	**1.00004**
3.0	1.9237	-	1.92368	**1.92358**
7.0 10.0	3.7207		3.07208	**3.07202**
	12.2940		12.2941	**12.2942**

As the mixed convection parameter G increases we observe that both the velocities increased and a reduction in temperature and concentration (Figs. 2a-2d). This may be on account of the difference between the wall temperature and ambient temperature is positive and due to its enhancement. Figures 3a –3d present the effect of magnetic parameter M on the non – dimensional primary velocity f'(η), secondary velocity g(η), temperature θ(η) and concentration φ(η). As the strength of the magnetic field increases, it is observed that there is a significant reduction in the primary velocity in other words, the primary flow is remarkably decelerated with stronger magnetic field intensity M due to the fact that the Lorentz force opposes the flow. The hydromagnetic drag force in (12) $-\frac{M}{1+m^2}(f'+mg)$ is proportionally increasing and thus this retarding force is enhanced significantly as M increases. As both the primary and secondary velocity components remain negative for all values of M, the collective effect of M is to generate a larger magnetic body force. However, the secondary velocity unlike the primary velocity increases in the region(0,1.0) and reduces in the region far away from the wall (fig.3b). The hydromagnetic drag force in (13) has two components, i.e, $-\frac{M}{1+m^2}(g+mf')$ consisting of a positive g (η) component and a negative component $f'(\eta)$. However, the later component has become a positive body force due to its multiple $-\frac{M}{1+m^2}$ and thus this primary flow becomes responsible to increase the secondary velocity for an enhancement in M.It is observed that (Fig. 3b) the point of maximum velocity in the secondary flow skews towards the surface for an increase in M. This can be attributed owing to the reduction in the thickness of the boundary layer with increasing M which in turn increases velocity gradient of the secondary flow in the vicinity of the surface. From Fig. 3d it is observed that enhancement of the magnetic field strength M results in the enhancement of temperature resulting from the heating effect of magnetic field. We observed that (Fig.3d) the volume fraction of nanoparticles enhances with rise in M.

The effect of Hall parameter m on the primary velocity, secondary velocity, temperature and concentration of the nanoparticle is presented in Figs.4a - 4d. It is observed that the primary velocity component and volume fraction of the nanoparticles increases while the secondary velocity and temperature decrease with increase in m due to the fact that increase in m results in reduction in magnetic damping which in turn increases the primary velocity and noapartivle concentration. As the buoyancy ratio increases we observe (Figs. 5a-5d) that both the velocity components, nanoparticle concentration decrease while the temperature enhances owing to the reduction in the temperature gradient.Figs.6a-6d represent the veration of velocity,temperature and concentration with thermal radiation parameter (Rd). From profiles we find that higher the radiative heat flux smaller the velocity components.Also for higher radiation parameter we notice an enhancement in temperature and depreciation in nanoparticle concentration. The impact of Nb, Nt qualitatively is same. The effect of the Brownian motion parameter and thermophoresis parameter is shown in Figs. 7a-7d & 8a-8d. The velocities decrease with Nb & Nt however, its influence on the primary, secondary velocity components is negligible. It is observed that the effect of the thermophoresis parameter is remarkable on the temperature and concentration of the nanoparticles as expected. As the thermophoresis parameter increases from 0.5 to 2 both the temperature as well as the nanoparticle concentration decrease significantly throughout the region. The Brownian motion parameter reduces the temperature and decreases concentration. Figs.9a-9b show the effect of slip parameter(A) on velocity,temperature and concentration.From the profiles we notice that an increase in A leads to a reduction in both the velocity components and concentration and enhances the temperature.This may be attributed to the fact that the thickness of the momentum and solutal boundary layer reduces with increase in slip parameter A while the thermal boundary layer increases with rise in A.Figs.10a-10d exhibit the effect of heat sources on the flow variables.The presence of heat generating/absorbing sources leads to an absorption on the heat energy which leads to a depreciation in velocity components,and concentration.The temperature reduces with rise in heat generating source and enhances with that of heat absorbing source.The effect of suction/injection on the velocity components ,temperature and concentration is illustrated in figs.11a-11d.An increase in suction parameter(fw>0) reduces both the velocities, concentration and enhances the temperature while the injection parameter(fw<0) reduces the velocities and enhances the temperature and concentration. Figs.12a-12d&13a-13d represent the effect of chemical reaction parameter(γ) on the flow variables.We find from the profiles 12a-12d that the velocities,temperature and nanoparticle concentration reduces in the flow region in the degenerating chemical reaction case(γ>0).while a reversed effect is noticed in the behaviour of

velocities, temperature and concentration in the case of generating case(figs.13a-13e)..The effect of Lewis number is shown in Figs. 14a-14d. With increase in Lewis number from 2 to 8 the primary and secondary velocities increase. However, there is a significant increase when Lewis number changes from 12a-12d. It can be seen from the profiles that the velocity and temperature enhances with raise in Le≤4 and reduces with higher rise in Le>6. The secondary velocity and nanoparticle concentration experience depreciation with increase in Le in the entire flow region (figs.12b&12d). There is a significant reduction in the concentration as Le changes from 2 to 6 an increase in Lewis number amounts to reduction in Brownian diffusion co-efficient. For a base fluid of certain kinematic viscosity ν, a higher Lewis number corresponds to a lower diffusion co-efficient DB which results in a smaller penetration depth for the concentration boundary layer. Fig. 15a-15d illustrates the effect of Prandtl number Pr on velocities, temperature and concentration profiles. It is noted that as Pr increases the both velocities,temperature and nanoparticle concentration decrease. This may be due to the reduction in the thermal diffusivity for increasing values of Pr which results in the decreasing of energy ability and as a result the thermal boundary layer reduces.

Variations of the local skin friction coefficient in the x – direction in terms of f " (0) , the skin friction coefficient in z – direction in terms of g ' (0) , the local Nusselt number in terms of – θ ' (0) and local Sherwood number in terms of – υ ' (0) are presented in table.2.It can be seen from the tabular values that an increase in Grashof number(G) enhances the skin friction in x and z-directions,Nusselt and Sherwood numbers on the wall.Higher the Lorentz force /Hall parameter (m) larger the skin friction components and Sherwood number and smaller the Nusselt number on the wall.The variation of τx, τz , Nu and Sh with buoyancy ratio(N) shows that when the molecular buoyancy force dominates over the thermal buoyancy force τx and Sh enhances while τz, Nu reduces on η=0 irrespective of the directions of the buoyancy forces. τx enhances and τz reduces on η=0 in both degenerating and generating chemical reaction cases while Nu and Sh enhance on the wall in the degenerating case and in generating case,Nu&Sh reduces on η=0. With respect to heat source,we find that τx and Nu reduces with increase in the strength of the heat generating source and increase with that of heat absorbing source while reversed effect is noticed in the case of τz and Nu.Higher the thermal radiation larger the skin friction components,Nusselt number and smaller the Sherwood number on the wall. An increase in Nb, Nt reduces the τx, Nu and enhances τz on the wall while Sh reduces with Nb and increases with Nt. τx increases, τz and Nu reduces with rise in suction/injection parameter (fw>0, fw<0) while Sh reduces with increase in suction parameter and increases with injection parameter (fw<0). Higher the values of slip parameter (A) larger the skin friction component τx and Sherwood number (Sh) on the wall. An increase in Le and Pr increases τx, Nu and reduces τz, Sh on η=0.

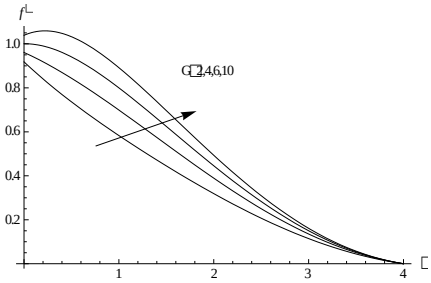

Fig.2a Effect of G on $f'(\eta)$
M=0.5, m=0.5, N=0.5, γ=0.5, Q1=0.5, Nr=0.5, Nt=0.5, Nb=0.5, B1=0.1, A=0.2,fw=0.2,Le=2, Pr=0.71

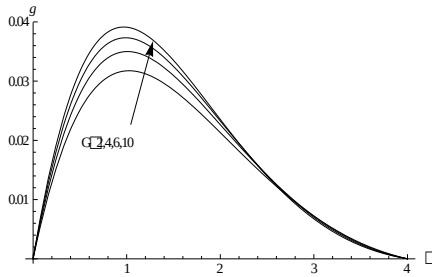

Fig.2b Effect of G on g(η)
M=0.5, m=0.5, N=0.5, γ=0.5, Q1=0.5, Nr=0.5, Nt=0.5, Nb=0.5, Q = 0.1, A=0.2,fw=0.2,Le=2, Pr=0.71

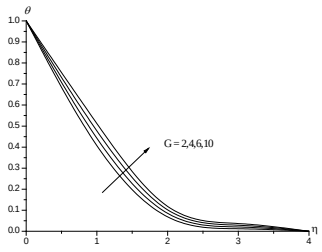

Fig.2c Effect of G on θ(η)
M=0.5, m=0.5, N=0.5, γ=0.5, Q1=0.5, Nr=0.5, Nt=0.5, Nb=0.5, Q=0.1, A=0.2,fw=0.2,Le=2, Pr=0.71

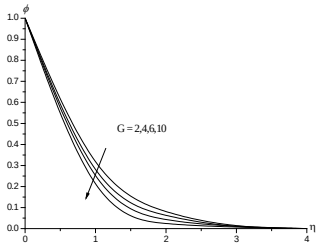

Fig.2d Effect of G on ϕ(η)
M=0.5, m=0.5, N=0.5, γ=0.5, Q1=0.5, Nr=0.5, Nt=0.5, Nb=0.5, Q=0.1, A=0.2,fw=0.2,Le=2, Pr=0.71

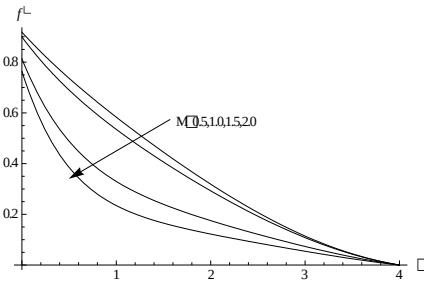

Fig.3a Effect of M on $f'(\eta)$
G=2, m=0.5, N=0.5, γ=0.5, Q1=0.5, Nr=0.5, Nt=0.5, Nb=0.5, Q=0.1, A=0.2,fw=0.2,Le=2, Pr=0.71

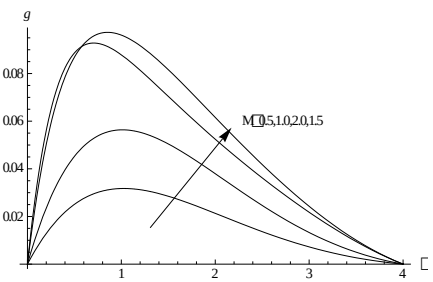

Fig.3b Effect of M on g(η)
G=2, m=0.5, N=0.5, γ=0.5, Q1=0.5, Nr=0.5, Nt=0.5, Nb=0.5,Q= 0.1, A=0.2,fw=0.2,Le=2, Pr=0.71

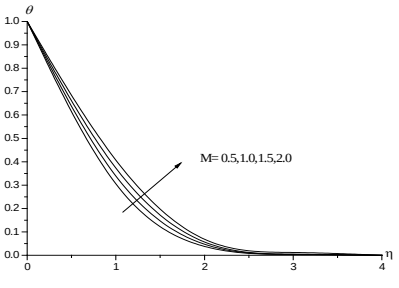

Fig.3c Effect of M on θ(η)
G=2, m=0.5, N=0.5, γ=0.5, Q1=0.5, Nr=0.5, Nt=0.5, Nb=0.5, Q=0.1, A=0.2,fw=0.2,Le=2, Pr=0.71

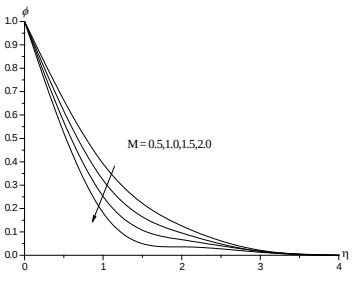

Fig.3d Effect of M on ϕ(η)
G=2, m=0.5, N= 0.5, γ=0.5, Q1=0.5, Nr=0.5, Nt=0.5, Nb=0.5, Q = 0.1, A=0.2,fw=0.2,Le=2, Pr=0.71

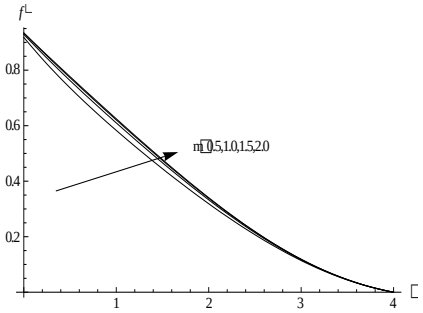

Fig.4a Effect of m on f' (η)
G=2,M=0.5, N=0.5, γ=0.5, Q1=0.5, Nr=0.5, Nt=0.5, Nb=0.5, Q=0.1, A=0.2,fw=0.2,Le=2, Pr=0.71

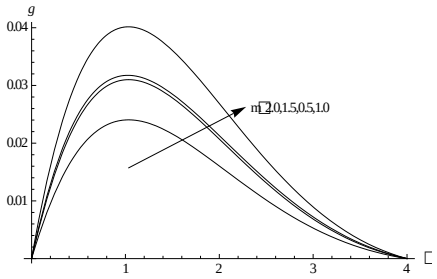

Fig.4b Effect of m on g(η)
G=2,M=0.5, N=0.5, γ=0.5, Q1=0.5, Nr=0.5, Nt=0.5, Nb=0.5, Q=0.1, A=0.2,fw=0.2,Le=2, Pr=0.71

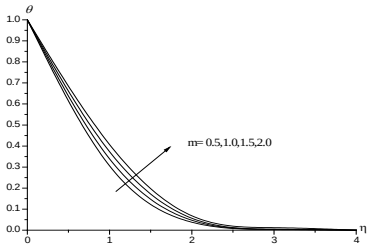

Fig.4c Effect of m on θ(η)
G=2,M=0.5, N=0.5, γ=0.5, Q1=0.5, Nr=0.5, Nt=0.5, Nb=0.5, Q=0.1, A=0.2,fw=0.2,Le=2, Pr=0.71

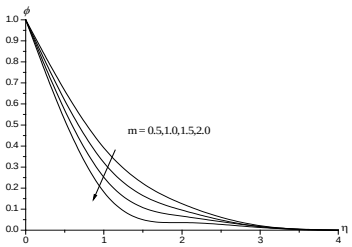

Fig.4d Effect of m on ϕ(η)
G=2,M=0.5, N=0.5, γ=0.5, Q1=0.5, Nr=0.5, Nt=0.5, Nb=0.5, Q=0.1, A=0.2,fw=0.2,Le=2, Pr=0.71

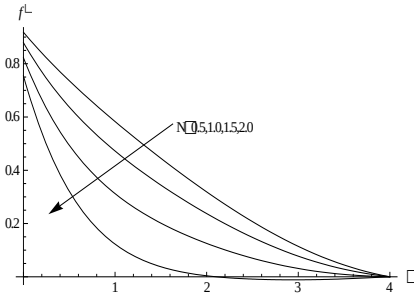

Fig.5a Effect of N on f' (η)
G=2,M=0.5, m=0.5, γ=0.5, Q1=0.5, Nr=0.5, Nt=0.5, Nb=0.5, Q=0.1, A=0.2,fw=0.2,Le=2, Pr=0.71

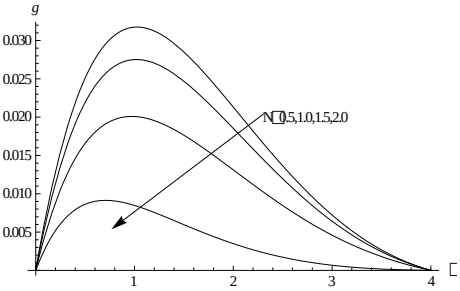

Fig.5b Effect of N on g(η)
G=2,M=0.5, m=0.5, γ=0.5, Q1=0.5, Nr=0.5, Nt=0.5, Nb=0.5, Q=0.1, A=0.2,fw=0.2,Le=2, Pr=0.71

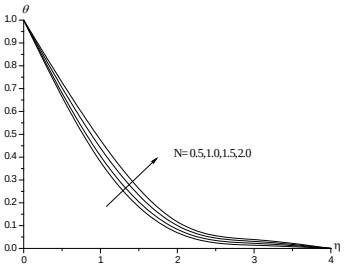

Fig.5c Effect of N on θ(η)
G=2,M=0.5, m=0.5, γ=0.5, Q1=0.5, Nr=0.5, Nt=0.5, Nb=0.5, Q=0.1, A=0.2,fw=0.2,Le=2, Pr=0.71

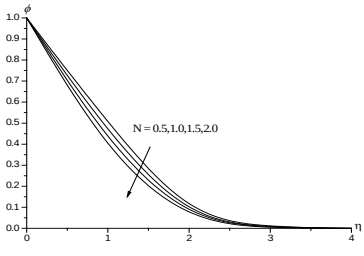

Fig.5d Effect of N on ϕ(η)
G=2,M=0.5, m=0.5, γ=0.5, Q1=0.5, Nr=0.5, Nt=0.5, Nb=0.5, Q=0.1, A=0.2,fw=0.2,Le=2, Pr=0.71

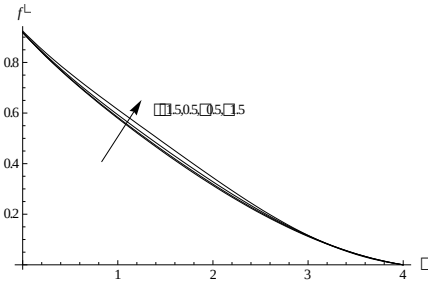

Fig.6a Effect of γ on f' (η)
G=2,M=0.5, m=0.5, N=0.5, Q1=0.5, Nr=0.5, Nt=0.5, Nb=0.5, Q=0.1, A=0.2,fw=0.2,Le=2, Pr=0.71

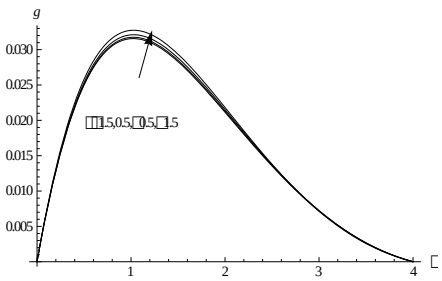

Fig.6b Effect of γ on g(η)
G=2,M=0.5, m=0.5, N=0.5, Q1=0.5, Nr=0.5, Nt=0.5, Nb=0.5, Q=0.1, A=0.2,fw=0.2,Le=2, Pr=0.71

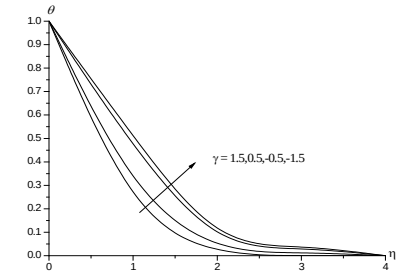

Fig.6c Effect of γ on θ(η)
G=2,M=0.5, m=0.5, N=0.5, Q1=0.5, Nr=0.5, Nt=0.5, Nb=0.5, Q=0.1, A=0.2,fw=0.2,Le=2, Pr=0.71

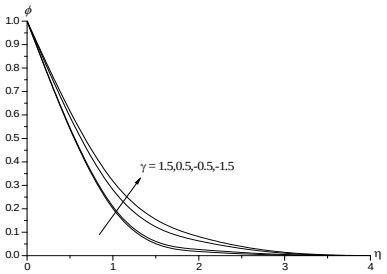

Fig.6d Effect of γ on ϕ(η)
G=2,M=0.5, m=0.5, N=0.5, Q1=0.5, Nr=0.5, Nt=0.5, Nb=0.5,Q=0.1, A=0.2,fw=0.2,Le=2, Pr=0.71

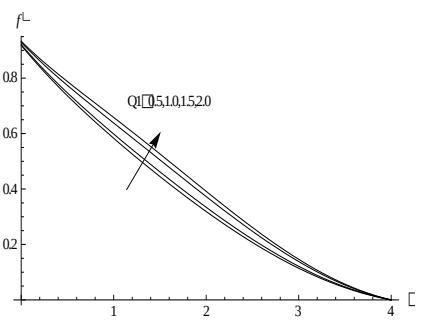

Fig.7a Effect of Q1 on f' (η)
G=2,M=0.5, m=0.5, N=0.5, γ=0.5, Nr=0.5, Nt=0.5, Nb=0.5, Q=0.1, A=0.2,fw=0.2,Le=2, Pr=0.71

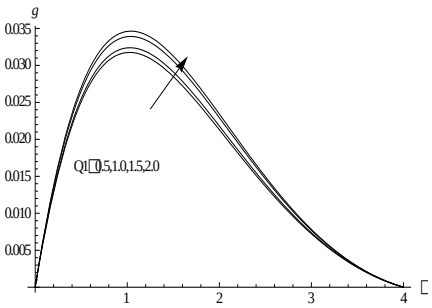

Fig.7b Effect of Q1 on g(η)
G=2,M=0.5, m=0.5, N=0.5, γ=0.5, , Nr=0.5, Nt=0.5, Nb=0.5,Q=0.1, A=0.2,fw=0.2,Le=2, Pr=0.71

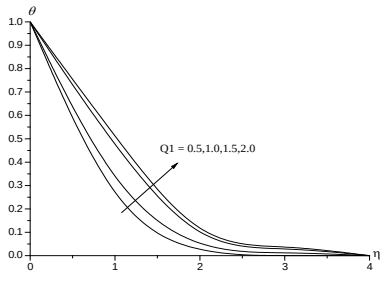

Fig.7c Effect of Q1 on θ(η)
G=2,M=0.5, m=0.5, N=0.5, γ=0.5, Nr=0.5, Nt=0.5, Nb=0.5,Q=0.1, A=0.2,fw=0.2,Le=2, Pr=0.71

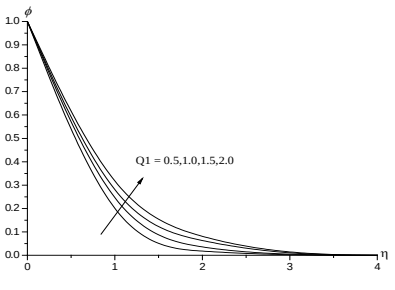

Fig.7d Effect of Q1 on ϕ(η)
G=2,M=0.5, m=0.5, N=0.5, γ=0.5, Nr=0.5, Nt=0.5, Nb=0.5, Q=0.1, A=0.2,fw=0.2,Le=2, Pr=0.71

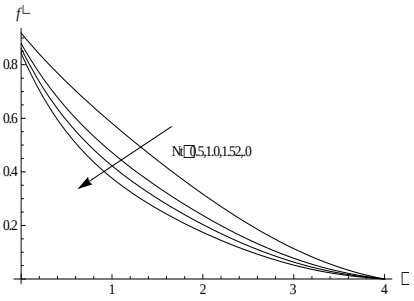

Fig.8a Effect of Nt on f' (η)
G=2,M=0.5, m=0.5, N=0.5, γ=0.5, Q1=0.5, Nr=0.5, Nb=0.5, Q=0.1, A=0.2,fw=0.2,Le=2, Pr=0.71

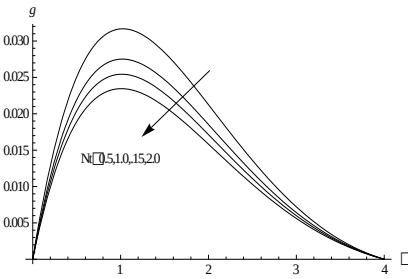

Fig.8b Effect of Nt on g(η)
G=2,M=0.5, m=0.5, N=0.5, γ=0.5, Q1=0.5, Nr=0.5, Nb=0.5, Q=0.1, A=0.2,fw=0.2,Le=2, Pr=0.71

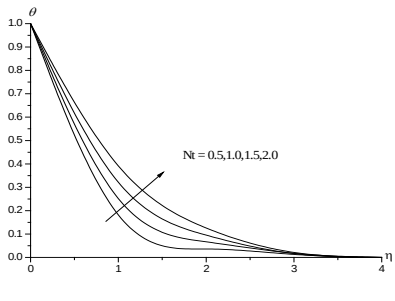

Fig.8c Effect of Nt on θ(η)
G=2,M=0.5, m=0.5, N=0.5, γ=0.5, Q1=0.5, Nr=0.5, Nb=0.5, Q=0.1, A=0.2,fw=0.2,Le=2, Pr=0.71

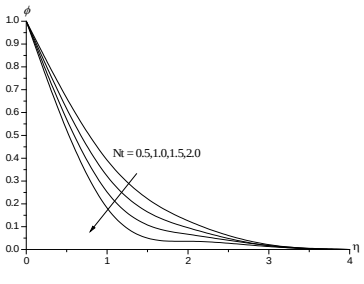

Fig.8d Effect of Nt on ϕ(η)
G=2,M=0.5, m=0.5, N=0.5, γ=0.5, Q1=0.5, Nr=0.5, Nb=0.5, Q=0.1, A=0.2,fw=0.2,Le=2, Pr=0.71

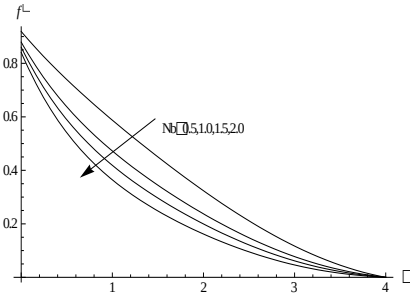

Fig.9a Effect of Nb on f' (η)
G=2,M=0.5, m=0.5, N=0.5, γ=0.5, Q1=0.5, Nr=0.5, Nt=0.5, Q=0.1, A=0.2,fw=0.2,Le=2, Pr=0.71

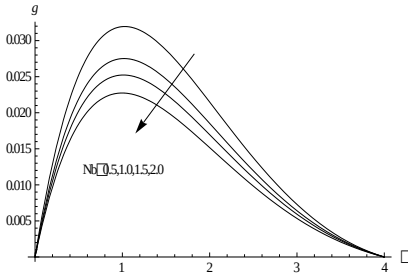

Fig.9b Effect of Nb on g(η)
G=2,M=0.5, m=0.5, N=0.5, γ=0.5, Q1=0.5, Nr=0.5, Nt=0.5, Q=0.1, A=0.2,fw=0.2,Le=2, Pr=0.71

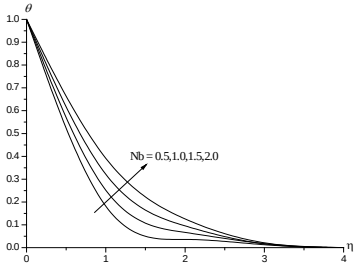

Fig.9c Effect of Nb on θ(η)
G=2,M=0.5, m=0.5, N=0.5, γ=0.5, Q1=0.5, Nr=0.5, Nt=0.5, Q=0.1, A=0.2,fw=0.2,Le=2, Pr=0.71

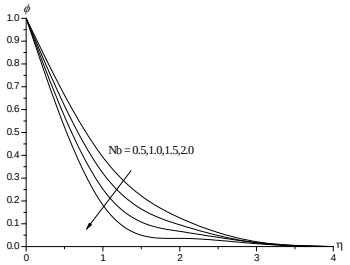

Fig.9d Effect of Nb on ϕ(η)
G=2,M=0.5, m=0.5, N=0.5, γ=0.5, Q1=0.5, Nr=0.5, Nt=0.5, Q=0.1, A=0.2,fw=0.2,Le=2, Pr=0.71

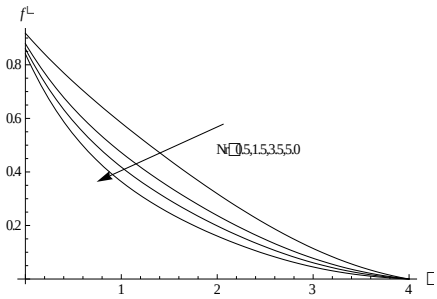

Fig.10a Effect of Nr on f' (η)
G=2,M=0.5, m=0.5, N=0.5, γ=0.5, Q1=0.5, Nt=0.5, Nb=0.5, Q=0.1, A=0.2,fw=0.2,Le=2, Pr=0.71

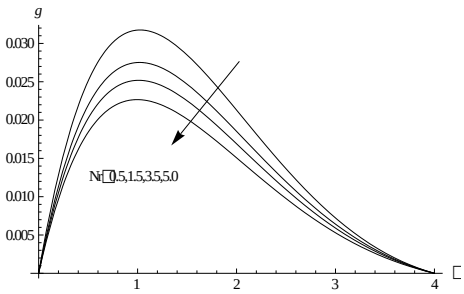

Fig.10b Effect of Nr on g(η)
G=2,M=0.5, m=0.5, N=0.5, γ=0.5, Q1=0.5, Nt=0.5, Nb=0.5, Q=0.1, A=0.2,fw=0.2,Le=2, Pr=0.71

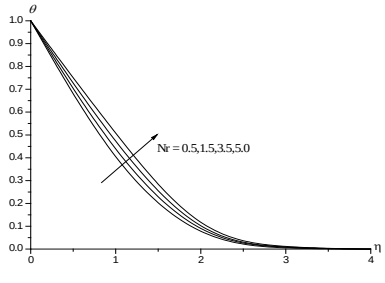

Fig.10c Effect of Nr on θ(η)
G=2,M=0.5, m=0.5, N=0.5, γ=0.5, Q1=0.5, Nt=0.5, Nb=0.5, Q=0.1, A=0.2,fw=0.2,Le=2, Pr=0.71

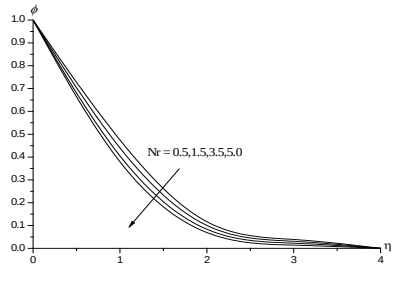

Fig.10d Effect of Nr on ϕ(η)
G=2,M=0.5, m=0.5, N=0.5, γ=0.5, Q1=0.5, Nt=0.5, Nb=0.5, Q=0.1, A=0.2,fw=0.2,Le=2, Pr=0.71

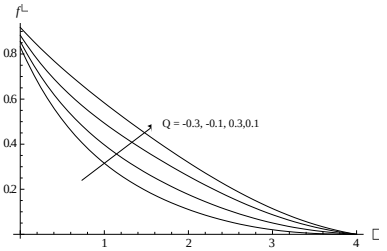

Fig.11a Effect of Q on $f'(\eta)$
G=2,M=0.5, m=0.5, N=0.5, γ=0.5, Q1=0.5, Nr=0.5, Nt=0.5, Nb=0.5, A=0.2,fw=0.2,Le=2, Pr=0.71

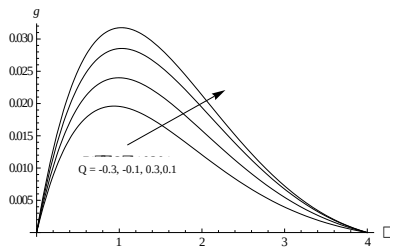

Fig.11b Effect of Q on g(η)
G=2,M=0.5, m=0.5, N=0.5, γ=0.5, Q1=0.5, Nr=0.5, Nt=0.5, Nb=0.5, A=0.2,fw=0.2,Le=2, Pr=0.71

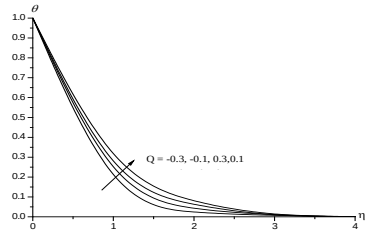

Fig.11c Effect of Q on θ(η)
G=2,M=0.5, m=0.5, N=0.5, γ=0.5, Q1=0.5, Nr=0.5, Nt=0.5, Nb=0.5, A=0.2,fw=0.2,Le=2, Pr=0.71

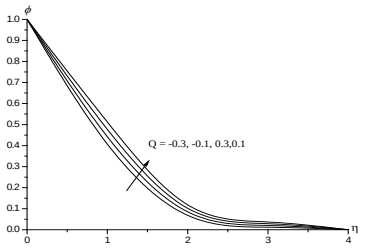

Fig.11d Effect of Q on ϕ(η)
G=2,M=0.5, m=0.5, N=0.5, γ=0.5, Q1=0.5, Nr=0.5, Nt=0.5, Nb=0.5, A=0.2,fw=0.2,Le=2, Pr=0.71

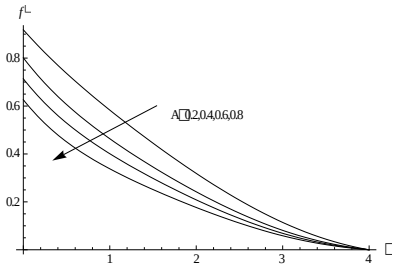

Fig.12a Effect of A on $f'(\eta)$
G=2,M=0.5, m=0.5, N=0.5, γ=0.5, Q1=0.5, Nr=0.5, Nt=0.5, Nb=0.5,Q=0.1, fw=0.2,Le=2, Pr=0.71

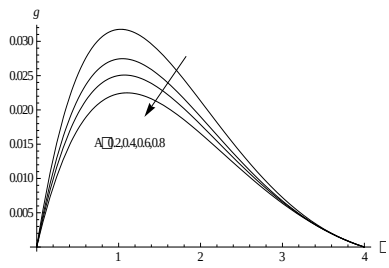

Fig.12b Effect of A on g(η)
G=2,M=0.5, m=0.5, N=0.5, γ=0.5, Q1=0.5, Nr=0.5, Nt=0.5, Nb=0.5, Q=0.1, fw=0.2,Le=2, Pr=0.71

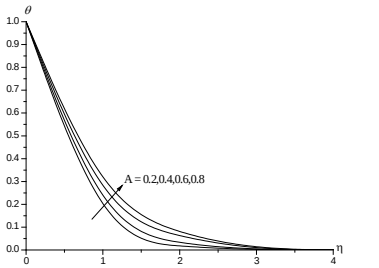

Fig.12c Effect of A on θ(η)
G=2,M=0.5, m=0.5, N=0.5, γ=0.5, Q1=0.5, Nr=0.5, Nt=0.5, Nb=0.5,Q=0.1, fw=0.2,Le=2, Pr=0.71

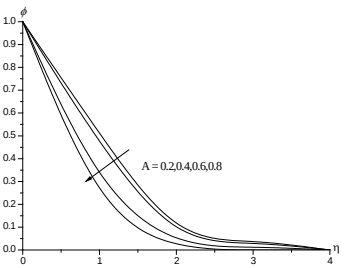

Fig.12d Effect of A on ϕ(η)
G=2,M=0.5, m=0.5, N=0.5, γ=0.5, Q1=0.5, Nr=0.5, Nt=0.5, Nb=0.5, Q=0.1, fw=0.2,Le=2, Pr=0.71

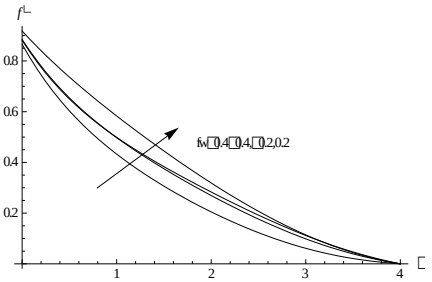

Fig.13a Effect of fw on $f'(\eta)$
G=2,M=0.5, m=0.5, N=0.5, γ=0.5, Q1=0.5, Nr=0.5, Nt=0.5, Nb=0.5, Q=0.1, A=0.2, Le=2, Pr=0.71

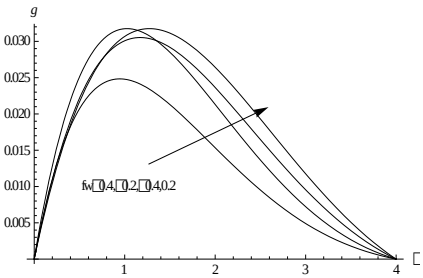

Fig.13b Effect of fw on g(η)
G=2,M=0.5, m=0.5, N=0.5, γ=0.5, Q1=0.5, Nr=0.5, Nt=0.5, Nb=0.5, Q=0.1, A=0.2, Le=2, Pr=0.71

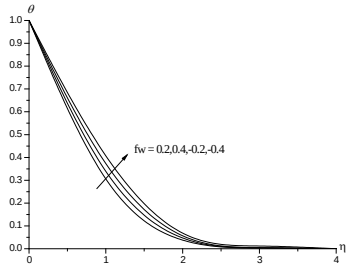

Fig.13c Effect of fw on θ(η)
G=2,M=0.5, m=0.5, N=0.5, γ=0.5, Q1=0.5, Nr=0.5, Nt=0.5, Nb=0.5, Q=0.1, A=0.2, Le=2, Pr=0.71

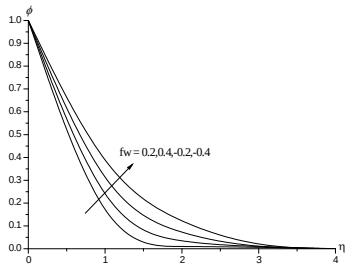

Fig.13d Effect of fw on ϕ(η)
G=2,M=0.5, m=0.5, N=0.5, γ=0.5, Q1=0.5, Nr=0.5, Nt=0.5, Nb=0.5,Q=0.1, A=0.2, Le=2, Pr=0.71

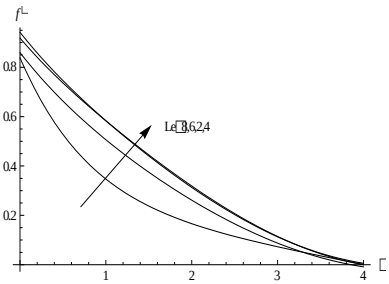

Fig.14a Effect of Le on $f'(\eta)$
G=2,M=0.5, m=0.5, N=0.5, γ=0.5, Q1=0.5, Nr=0.5, Nt=0.5, Nb=0.5,Q=0.1, A=0.2,fw=0.2, Pr=0.71

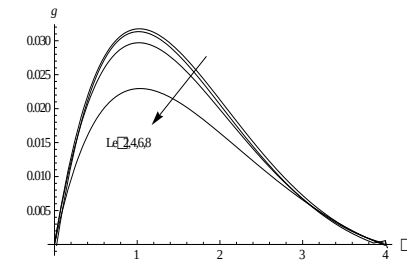

Fig.14b Effect of Le on g(η)
G=2,M=0.5, m=0.5, N=0.5, γ=0.5, Q1=0.5, Nr=0.5, Nt=0.5, Nb=0.5, Q=0.1, A=0.2,fw=0.2, Pr=0.71

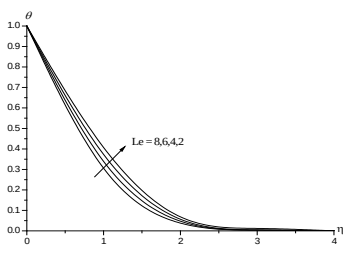

Fig.14c Effect of Le on θ(η)
G=2,M=0.5, m=0.5, N=0.5, γ=0.5, Q1=0.5, Nr=0.5, Nt=0.5, Nb=0.5, Q=0.1, A=0.2,fw=0.2, Pr=0.71

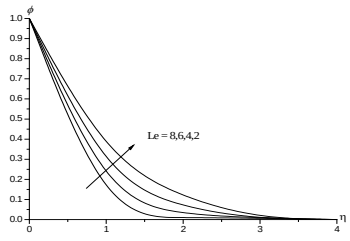

Fig.14d Effect of Le on ϕ(η)
G=2,M=0.5, m=0.5, N=0.5, γ=0.5, Q1=0.5, Nr=0.5, Nt=0.5, Nb=0.5, Q=0.1, A=0.2,fw=0.2, Pr=0.71

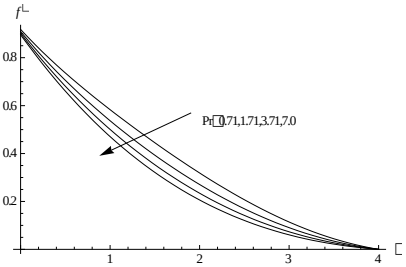

Fig.15a Effect of Pr on f' (η)
G=2,M=0.5, m=0.5, N=0.5, γ=0.5, Q1=0.5, Nr=0.5, Nt=0.5, Nb=0.5, Q=0.1, A=0.2,fw=0.2,Le=2

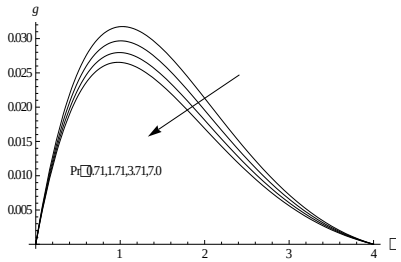

Fig.15b Effect of Pr on g(η)
G=2,M=0.5, m=0.5, N=0.5, γ=0.5, Q1=0.5, Nr=0.5, Nt=0.5, Nb=0.5, Q=0.1, A=0.2,fw=0.2,Le=2

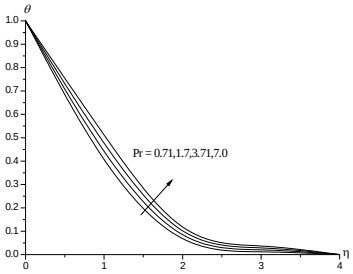

Fig.15c Effect of Pr on θ(η)
G=2,M=0.5, m=0.5, N=0.5, γ=0.5, Q1=0.5, Nr=0.5, Nt=0.5, Nb=0.5, Q=0.1, A=0.2,fw=0.2,Le=2

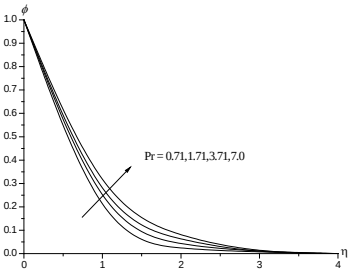

Fig.15d Effect of Pr on ϕ(η)
G=2,M=0.5, m=0.5, N=0.5, γ=0.5, Q1=0.5, Nr=0.5, Nt=0.5, Nb=0.5, Q=0.1, A=0.2,fw=0.2,Le=2

Table-2: Skin friction components, Nusselt and Sherwood number at η=0

Parameter		**τx(0)**	**τz(0)**	**Nu(0)**	**Sh(0)**
G	**2**	-0.408571	0.075298	0.242568	0.468033
	4	0.330863	0.08882	0.271606	0.429917
	6	0.368168	0.0984364	0.294653	0.401826
	10	1.01391	0.112411	0.332546	0.359808
M	**0.5**	-0.408571	0.075298	0.242568	0.468033
	1.0	-0.502937	0.139568	0.236055	0.477432
	1.5	-0.932526	0.322962	0.207385	0.522585
	2.0	-1.17852	0.385292	0.193509	0.548006
m	**0.5**	-0.408571	0.075298	0.242568	0.468033
	1.0	-0.391738	0.0923709	0.243685	0.466428
	1.5	-0.354416	0.0931466	0.246219	0.462841
	2.0	-0.334241	0.113575	0.248438	0.460416
N	**0.5**	-0.408571	0.075298	0.242568	0.468033
	1.0	-0.503159	0.0713651	0.235144	0.478105
	1.5	-0.603087	0.0670103	0.22729	0.489179
	2.0	-0.698985	0.0626117	0.220354	0.499872
γ	**0.5**	-0.408571	0.075298	0.242568	0.468033
	1.5	-0.410913	0.0750336	0.275911	0.998019
	-0.5	-0.399802	0.0758929	0.174276	-0.143159
	-1.5	-0.379583	0.077052	0.0518587	-0.844062
Q1	**0.5**	-0.408571	0.075298	0.242568	0.468033
	1.0	-0.353659	0.0788847	0.1550789	0.574413
	1.5	-0.311124	0.0814024	-0.107581	0.672301
	2.0	-0.276989	0.0832709	-0.05215	0.764138

Parameter		τx(0)	τz(0)	Nu(0)	Sh(0)
Nr	**0.5**	-0.408571	0.075298	0.242568	0.468033
	1.0	-0.391779	0.076447	0.189165	0.496904
	1.5	-0.376313	0.0775022	0.141933	0.520926
	2.0	-0.369043	0.077996	0.120245	0.531504
Nt	**0.5**	-0.409877	0.0752022	0.245873	0.46311
	1.5	-0.408571	0.075298	0.242568	0.468033
	3.5	-0.406849	0.0754249	0.238453	0.477199
	5.0	-0.405607	0.0755183	0.235849	0.486287
Nb	**0.5**	-0.409571	0.0752203	0.246122	0.473391
	1.0	-0.408571	0.0752981	0.242568	0.468033
	1.5	-0.407149	0.0754036	0.237848	0.46606
	2.0	-0.406131	0.0754798	0.234547	0.465101
Q	**0.1**	-0.408571	0.0752982	0.242568	0.468033
	0.3	-0.393441	0.0763036	0.192846	0.495759
	-0.1	-0.421918	0.0743978	0.286927	0.442712
	-0.3	-0.434777	0.0735189	0.330208	0.417453
A	**0.2**	-0.408571	0.0752982	0.242568	0.468033
	0.4	-0.319334	0.0736556	0.239862	0.474067
	0.6	-0.266847	0.0726596	0.238232	0.477739
	0.8	-0.229481	0.0719154	0.237763	0.480034
fw	**0.2**	-0.408571	0.0752982	0.242568	0.468033
	0.4	-0.459025	0.0765129	0.246883	0.412954
	-0.2	-0.328837	0.0716689	0.235795	0.595652
	-0.4	-0.291633	0.0689821	0.233289	0.684017
Le	**2**	-0.408571	0.075298	0.242568	0.468033
	4	-0.439831	0.0729377	0.295729	0.175492
	6	-0.448311	0.0673339	0.250421	-0.00723585
	8	-0.620374	0.0603844	0.122301	-0.00135594
Pr	**0.71**	-0.408571	0.0752982	0.242568	0.468033
	1.71	-0.453376	0.0720054	0.380943	0.392912
	3.71	-0.489606	0.0693082	0.502524	0.319375
	7.00	-0.520958	0.0669689	0.617184	0.244152

4. CONCLUSION

In this paper a mathematical model has been proposed to study the effect of Hall current on the boundary layer flow and heat transfer of a nanofluid over a stretching sheet. The fluid is subjected to a strong transverse magnetic field applied perpendicularly to the sheet assuming the magnetic Reynolds number is small. Using similarity variables the governing partial differential equations have been transformed into non-linear ordinary differential equation. The fourth order Runge-Kutta scheme with shooting method is employed to solve these equations for different values of the governing parameters. The influence of physical parameters on the velocity, temperature, nano particle volume fraction including the local skin friction coefficient as well as the local Nusselt number and Sherwood number is illustrated graphically.

1. The effect of Hall parameter m is to enhance the width of the boundary layer region, heat transfer rate, local skin friction coefficient and local Sherwood number for the primary flow. For the secondary flow a reduction in the skin friction is observed. The thickness of the thermal boundary layer and concentration boundary layer is reduced.
2. The magnetic field is observed to produce exactly an opposite effect to that of the Hall parameter on all the flow variables viz. primary and secondary velocities, temperature and concentration, skin friction, Nusselt number, Sherwood number on the stretching sheet.

3. The variation of Prandtl number produces a smaller velocity boundary layer thickness than that of the thermal boundary layer. It is also observed that for higher Prandtl number the thermal boundary layer is thinner than at a smaller Prandtl number.
4. The enhancement in Brownian motion and thermophoresis parameters produce a larger thermal boundary layer thickness than the hydrodynamic boundary layer thickness. The Brownian motion parameter decreases the volume fraction while an opposite effect is observed with thermophoresis parameter.

5. REFERENCES

1. Abd El-Aziz, M., Flow and heat transfer over an unsteady stretching surface with Hall effect, Meccanica 45, 97-109 (2010).
2. Abo-Eldahab, E. M., Abd El Aziz, M., Hall and ion-slip effect on MHD free convective heat generating flow past a semi-infinite vertical flat plate, Phs. Scripta 61 (2000) 344.
3. Abo-Eldahab, E. M., Elbarbary, M. E., Hall current effect on magnetohydrodynamic free-convection flow past a semi-infinite vertical plate with masstransfer, Int. J. Eng. Sci. 39 (2001) 1641.
4. Abo-Eldahab, E. M., Salem, A. M., Hall effects on MHD free convection flow of a non- Newtonian power-law fluid at a stretching surface, Int. Commun. Heat Mass 31(3), 343- 354 (2004)
5. Ali, F. M., Nazar, R., Arifin, N. M., and Pop, I., Effect of Hall current on MHD mixed convection boundary layer flow over a stretched vertical flat plate, Meccanica 46, 1103- 1112 (2011).
6. Ali, M. E., Heat Transfer characteristics of a continuous stretching surface, Warme-und Stoffubertragung 29(4), 227-234 (1994).
7. Bachok, N., Ishak, A., Pop, I., Boundary-layer flow of nanofluids over a moving surface in a flowing fluid, International journal of thermal sciences, vol.49, pp.1663-1668, 2010.
8. Buongiorno, J., Convective transport in nanofluids, J. Heat Transfer 128 (2006) 240 – 250.
9. Chamkha, A. J., Aly, A. M., and Al – Mudhaf, H., Int. J. Microscale Nanoscale Thermal Fluid Transp. Phenom. 2, 51 (2011).
10. Choi, S. U. S., Zhang, Z. G., Yu, W., Lockwood, F. E., and Grulke, E. A., Anomalous thermal conductivity enhancement in nano – tube suspensions, Appl. Phys. Lett., 79, (2001) 2252 – 2254.
11. Choi, S.U.S., Enhancing thermal conductivity of fluids with nanoparticles, Developments and Applications of Non-Newtonian Flows, FED-vol. 231/MD-vol. 66, 1995, pp. 99-105.
12. Crane, LJ (1970), Flow past a stretching sheet, J. Appl. Math. Phys. (ZAMP) 21: 645 – 647.
13. Eastman, J. A., Choi, S. U. S., Li, S., Thompson, L. J., and Lee, S., Enhanced thermal conductivity through the development of nanofluids, in: Nanophase and Nanocomposite Materials II, eds. S. Komarneni, J. C. Parker and H. J. Wollenberger, pp. 3 – 11 (1997), Materials Research Society, Pittsburgh.
14. Eastman, J. A., Choi, S. U. S., Li, S., Yu, W., Thompson, L. J., Anomalously increased effective thermal conductivity of ethylene glycol – based nanofluids containing copper nanoparticles, Appl. Phys. Lett., 78(6) : (2001) 718 – 720.
15. Gorla, R. S. R. O., and Chamkha, A., Natural convective boundary layer flow over a horizontal plate embedded in a porous medium saturated with a nanofluid, Journal of Modern Physics, vol. 2, pp. 62 – 71, 2011.
16. Grubka, L. J., and Bobba, K. M., Heat Transfer characteristics of a continuous, stretching surface with variable temperature, J. Heat Transf. 107(1), 248-250 (1985)
17. Hamad, M. A. A., Ferdows, M., Similarity solution of boundary layer stagnation – point flow towards a heated porous stretching sheet saturated with a nanofluid with heat absorption/generation and suction/blowing: a lie group analysis. Commun Nonlinear Sci Numer Simulat 2011, 17(1) : 132 – 140.
18. Hamad, M.A., Pop, I., Ismail, A.I., Magnetic field effects on convection flow of a nanofluid past a vertical semi-infinite flat plate, Non-Linear Analysis: Real World Applications, vol.12, pp.1338-1346, 2011.
19. Keblinski, P., Phillpot, S. R., Choi, S. U. S., and Eastman, J. A., Mechanisms of heat flow in suspensions of nano – sized particles (nanofluids), Int. J. Heat and Mass Trans, 45(4), 855 - 863 (2002).
20. Khan, M. S., Karim, I., Ali, L. E., Islam, A., Unsteady MHD free convection boundary- layer flow of a nanofluid along a stretching sheet with thermal radiation and viscous dissipation effects, Int. Nano Lett. 2, 24 (2012)
21. Khan, WA, Pop, I, Boundary-layer flow of a nanofluid past a stretching sheet. Int. J Heat Mass Transf 53 (2010) 24772483
22. Kleinstreue, C., J. Li and J. Koo, Microfluidics of nano-drug delivery, Int. J. Heat and Mass Transf. 51(23), 5590-5597 (2008).
23. Kuznetsov, A. V., Nield, D. A., Natural convective boundary-layer flow of ananofluid past avertical plate, Int. J. Therm. Sci. 49 (2010) 243 – 247.
24. Makinde, O. D., Aziz, A., Boundary layer flow of a nanofluid past a stretching sheet with convective boundary condition, Int. J. Therm. Sci. 50 (2011) 1326 – 1332.
25. Makinde, O. D., Aziz, A., Boundary layer flow of a nanofluid past a stretching sheet with convective boundary condition, Int. J. of Therm. Sci. 50 (2011) 1326 – 1332.
26. Minsta, H. A., Roy, G., Nguyen, C. T., Doucet, D., New temperature dependent thermal conductivity data for water – based nanofluids, Int. J. Thermal Sci. 48 : (2009) 363 – 371.

27. Mohamed Abd El-Aziz, Effects of Hall current on the flow and heat transfer of a nanofluid over a stretching sheet with partial slip, International Journal of Modern Physics C, Vol. 24, No. 7 (2013) 1350044.
28. Nadeem, S., Lee, C., Boundary layer flow of a nanofluid over an exponentially stretching surface. Nanoscale Res Lett 2012, 7:94.
29. Rana, P., Bhargava, R., Flow and heat transfer of a nanofluid over a nonlinearly stretching sheet: A numerical study, Communications in Nonlinear Science and Numerical Simulation, 2011.
30. Sutton, G. W., Sherman, A., Engineering Magnetohydrodynamics, Mc Graw- Hill, ew York, (1965)
31. Xiaohonh Su, Liancun Zheng, Hall effect on MHD flow and heat transfer of nanofluids over a stretching wedge in the presence of velocity slip and Joule heating, Cent. Eur. J. Phys. 11(12) . 2013.1694 – 1703.

Source of support: Nil, Conflict of interest: None Declared.